Induction of p21CIP1 Protein and Cell Cycle Arrest after Inhibition of Aurora B Kinase Is Attributed to Aneuploidy and Reactive Oxygen Species*[S]

Geeta Kumari[‡1], **Tanja Ulrich**[‡], **Michael Krause**[§], **Florian Finkernagel**[§], and **Stefan Gaubatz**[‡2]

From the ‡Theodor Boveri Institute, Biocenter, University of Wuerzburg and Comprehensive Cancer Center Mainfranken, 97080 Wuerzburg, Germany and the §Institute for Molecular Biology and Tumor Research (IMT), University of Marburg, Emil-Mannkopffstrasse 2, 35033 Marburg, Germany

Background: p21 is induced when Aurora B is inhibited.
Results: p21-induction after Aurora B inhibition is attributed to aneuploidy and reactive oxygen species.
Conclusion: Aneuploidy and ROS mediate cell cycle arrest after Aurora B inhibition by promoting p21-induction.
Significance: The study contributes to the understanding of the mechanisms for p21-induction and cell cycle arrest following an aberrant mitosis.

Cell cycle progression requires a series of highly coordinated events that ultimately lead to faithful segregation of chromosomes. Aurora B is an essential mitotic kinase, which is involved in regulation of microtubule-kinetochore attachments and cytokinesis. Inhibition of Aurora B results in stabilization of p53 and induction of p53-target genes such as p21 to inhibit proliferation. We have previously demonstrated that induction of p21 by p53 after inhibition of Aurora B is dependent on the p38 MAPK, which promotes transcriptional elongation of p21 by RNA Pol II. In this study, we show that a subset of p53-target genes are induced in a p38-dependent manner upon inhibition of Aurora B. We also demonstrate that inhibition of Aurora B results in down-regulation of E2F-mediated transcription and that the cell cycle arrest after Aurora B inhibition depends on p53 and pRB tumor suppressor pathways. In addition, we report that activation of p21 after inhibition of Aurora B is correlated with increased chromosome missegregation and aneuploidy but not with binucleation or tetraploidy. We provide evidence that p21 is activated in aneuploid cells by reactive oxygen species (ROS) and p38 MAPK. Finally, we demonstrate that certain drugs that act on aneuploid cells synergize with inhibitors of Aurora B to inhibit colony formation and oncogenic transformation. These findings provide an important link between aneuploidy and the stress pathways activated by Aurora B inhibition and also support the use of Aurora B inhibitors in combination therapy for treatment of cancer.

Precise regulation of mitosis is important to ensure accurate segregation of duplicated chromosomes to daughter cells.

Defects in mitotic fidelity cause chromosome segregation errors and aneuploidy, a hallmark of human tumors (1).

Aurora kinases are mitotic kinases that play key roles in mitosis (2–4). Aurora B is the catalytic subunit of the chromosomal passenger complex (CPC),[3] which also contains the non-catalytic subunits INCENP (Inner Centromere Protein), Survivin, and Borealin. The CPC shows a characteristic pattern of association with chromatin in prophase and centromeric localization in prometaphase and metaphase. In late anaphase and telophase it transfers to the midzone and midbody (5). One of the key functions of the CPC is to regulate chromosome segregation by promoting the correct attachment of the mitotic spindle and by destabilizing defective microtubule-chromosome attachments (6). In addition the CPC also plays a crucial role in cytokinesis, the final process of cell division at the end of mitosis. Inactivation of Aurora B causes cytokinesis failure resulting in premature exit from mitosis without cell division (7–9). After failure of cytokinesis, cells arrest as 4N cells in G1 phase of the subsequent cell cycle. The cyclin-dependent kinase inhibitor p21, a p53-target gene, plays a critical role in mediating growth arrest upon inhibition of Aurora B (7, 8, 10). The expression of p21 is primarily controlled at the transcriptional level. The p21 gene contains high levels of paused RNA polymerase II at the promoter in the uninduced state (11–13). This allows for rapid induction of p21 after p53 activation. We have recently shown that induction of p21 after inhibition of Aurora B depends on p38 MAPK signaling (10). We found that p38 is not required for stabilization of p53 or for binding of p53 to the p21 promoter but that it instead promotes transcriptional elongation of p21 by RNA Pol II in response to Aurora B inhibition.

How p38 signaling is activated in response to Aurora B inhibition has not been addressed. Because it has been suggested that a tetraploidy checkpoint arrests cells in G1 after mitotic slippage or cytokinesis failure (14, 15), activation of p38 could be related to this proposed checkpoint. The tetraploidy-check-

---

[S] This article contains supplemental data S1 and S2.

[3] The abbreviations used are: CPC, chromosomal passenger complex; ROS, reactive oxygen species; RB, retinoblastoma.

point was proposed to detect an increase in chromosome number and to arrest the cells in a tetraploid G1 state. However, the concept of a true tetraploidy-checkpoint has recently been challenged (16, 17). Other possibilities that have been proposed to mediate the cell cycle arrest after an aberrant mitosis include DNA-damage, centrosomal stress, or activation of p53 by the lack of transcription during prolonged mitosis (18–20).

In this study we have ascertained the mechanisms underlying activation of p38 and induction of p21 in response to inhibition of Aurora B. We report that activation of p38 and p21 does not require tetraploidy but is correlated with aneuploidy. Further, we provide evidence that p38 and p21 are activated in aneuploid cells due to reactive oxygen species (ROS) but not by DNA-damage. Finally, we demonstrate that drugs that act on aneuploid cells synergize with inhibitors of Aurora B to inhibit colony formation and oncogenic transformation.

EXPERIMENTAL PROCEDURES

Cell Culture—U2OS and HCT116 cells were cultured in DMEM (Invitrogen) containing 10% FCS (Invitrogen). Cells were treated with the indicated concentrations of ZM447439 (Enzo), SB202190 (Sigma), AZD1152 (Selleckchem), thymidine (Sigma), 17-AAG (Biomol), 5-aminoimidazole-4-carboxamide 1-β-D-ribofuranoside (AICAR, Biomol), VE-821 (Tinib-Tools), KU5593 (Selleck), 4,5-dihydroxybenzene-1,3-disulfonate (Tiron) (Invitrogen).

Immunofluorescence—Cells grown on coverslips were fixed for 10 min at room temperature with PFA (PBS, 3% paraformaldehyde, 2% sucrose). PFA-fixed cells were permeabilized for 5 min with 0.2% Triton-X-100 in PBS and washed with PBST (0.1% Triton X-100 in PBS). Slides were blocked for 60 min with 2% BSA in PBS, washed three times in PBS and incubated with primary antibodies. Coverslips were washed three times with PBS and incubated with secondary antibody (Invitrogen) in PBST for 30 min. Nuclei were stained with Hoechst 33258 (Sigma).

Colony Formation Assay—For colony formation assays, 700 cells were plated on 6-well dishes and treated with the indicated drugs. 14 days later, cells were fixed and stained with crystal violet.

FACS Analysis—For FACS analysis cells were stained with propidium iodide and analyzed on a Beckman Coulter FC500.

Antibodies—The following primary antibodies were used: p21 (sc-397, Santa Cruz Biotechnology), p38 and phospho-p38 (Thr-180/Tyr-182) (Cell Signaling), p53 (DO-1, sc-126, Santa Cruz), pRB (C-15, Santa Cruz Biotechnology), β-actin (sc-47778, Santa Cruz Biotechnology), tubulin (Sigma), pATM/ATR-substrate (Cell Signaling), γH2AX (Millipore), SV40 large T (Pab 108, sc-148, Santa Cruz Biotechnology), phospho-Chk1 (Ser-345) (Cell Signaling), phospho-Chk2 (Thr-68) (Cell Signaling).

Immunoblotting—Cells were lysed in TNN (50 mM Tris, pH 7.5, 120 mM NaCl, 5 mM EDTA, 0.5% Nonidet P-40, 10 mM $Na_4P_2O_7$, 2 mM Na_3VO_4, 100 mM NaF, 10 mg/ml phenylmethylsulfonyl fluoride, protease inhibitors (Sigma)). Proteins were separated by SDS-PAGE, transferred to PVDF membrane, and detected by immunoblotting.

Soft Agar Assays—HCT116 cells seeded in 6-cm dishes were treated with ZM447439 and AICAR as indicated. Three days later, 1×10^4 cells were transferred to 2 ml of DMEM containing 0.35% low-gelling agarose (containing the respective drugs) and seeded in triplicate into 6-well plates containing a 2-ml layer of solidified 0.7% agarose in complete medium. After 13 days, the number of foci was scored.

Interphase FISH—For FISH in interphase cells, poseidon chromosome 7 and 8 satellite enumeration probes (Kreatech Diagnostics) were used according to the manufacturer. DNA was counterstained with Hoechst 33258. Fluorescence signals of at least 650 nuclei were counted.

ROS Detection—For the detection of ROS, cells grown on coverslips were washed once with warm PBS and incubated with 10 μM 2'-7'-dichlorodihydrofluorescein diacetate (H2DCF-DA, Molecular Probes) in PBS. After 10 min at 37 °C, the H2DCF-DA solution was removed, and the cells were incubated for 10 min with complete medium at 37 °C. Cells were washed again with warm PBS and fixed in 4% formalin (Applichem). Nuclei were counterstained with Hoechst 33258. For detection with MitoSox Red (Molecular Probes), cells grown on coverslips were washed once with warm PBS and incubated for 10 min with 5 μM MitoSox Red (Molecular Probes) in PBS at 37 °C. Cells were washed three times with PBS, and nuclei were counterstained with Hoechst 33342 for 20 min. Intracellular ROS levels were visualized using an inverted microscope.

Microarray—Using the two color Quick-Amp Labeling Kit (Agilent) 1 μg of total RNA was used for cDNA synthesis, mRNA amplification and labeling according to manufacturer's instructions. Transcriptional profiling was done on an oligonucleotide array (Agilent) and analyzed as described before. Expression data and gene annotations were stored in Array Express (accession: E-MTAB-1210), which complies with MIAME (minimal information about a microarray experiment) guidelines. For experimental comparisons, genes showing at least a 2-fold change were chosen. To identify genes that depend on p38-signaling for their induction, genes whose expression levels were lowered by SB202190 by $\log_2 > 0.5$ relative to expression in cells treated with ZM4474439 alone were identified.

RESULTS

A Subset of p53 Target Genes Induced after Inhibition of Aurora B Are Dependent on p38 Signaling—We and others have recently shown that inhibition of the mitotic kinase Aurora B results in induction of the CDK inhibitor p21 (8, 10, 21–25). Experiments with pharmacological inhibitors, isogenic cell lines, and specific siRNAs demonstrated that induction of p21 in response to Aurora B inhibition requires p53 as well as the MAPK p38 (10). We have also shown that while binding of p53 to the p21 promoter is p38-independent, p38 is required for transcriptional elongation of p21 in response to Aurora B inhibition (10).

To investigate whether, in addition to p21, other genes also require p38-signaling when Aurora B is inhibited, we performed microarray analysis after Aurora B inhibition in the presence and absence of p38 MAPK signaling. To do so, we treated U2OS cells with ZM447439, a selective pharmacologi-

A

	upregulated	downregulated
# total	730	418
# p38 independent	374	198
# p38 dependent	356	220

B p53 target genes induced by ZM447439 in a p38 dependent manner

Gene Symbol	Induction by ZM	% expr. with SB
TNFSF7	3.31	39.96
ATF3	2.63	50.76
SORCS3	2.50	52.00
ANK1	2.50	52.51
BBC3	5.86	54.71
FDXR	3.22	60.48
CYP4F3	2.62	63.02
SERPINB5	3.16	63.29
IER3	2.08	63.64
CDKN1A	4.06	65.52
TP53I3	2.64	65.98
PPM1D	2.30	68.78
ZMAT3	3.10	68.78
KAI1	2.35	69.26
DDB2	2.01	70.71

D
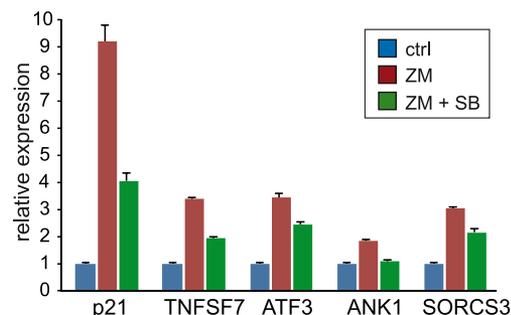
C p53 target genes induced by ZM447439 in a p38-independent manner

Gene Symbol	Induction by ZM	% expr. with SB
SESN1	4.17	122.26
SERPINE1	3.46	119.75
WNK1	2.33	100.00
FBXW7	2.25	92.02
GDF15	7.21	92.02
RRM2B	3.51	91.38
MDM2	4.53	90.75
FAS	4.08	88.27
TRIM22	2.41	88.27
PHLDA3	2.14	86.45
FHL2	3.56	86.45
BTG2	4.00	81.79
SESN2	2.41	81.23
TRIAP1	2.57	79.55

E
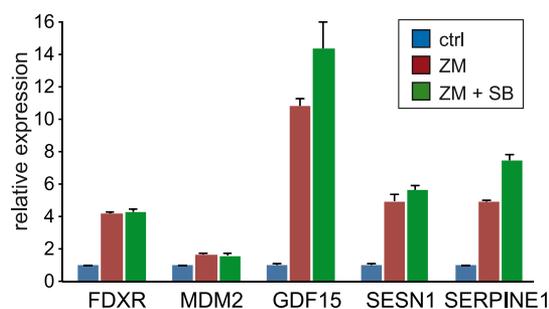
FIGURE 1. **Activation of a subset of p53 target genes due to Aurora B inhibition requires p38 signaling.** *A*, microarray analysis of U2OS cells pretreated with DMSO or 10 μM SB202190 for 2 h followed by treatment with 1 μM ZM447439 for 36 h. RNA was isolated and subjected to microarray analysis. The table shows the number of genes up-regulated or down-regulated more than 2-fold. *B* and *C*, p53 target genes that are induced by ZM447439 at least 2-fold and that are either dependent (*B*) or independent (*C*) on p38. The column % expr. with SB compares induction by ZM447439 in the absence of SB202190 with induction in the presence of SB202190. *D* and *E*, validation of microarray data. U2OS cells were treated as above. mRNA levels of the indicated p38-dependent (*D*) and independent (*E*) p53 target genes were determined by RT-qPCR.

cal Aurora B inhibitor. To explore whether p38 MAPK is involved in the response to Aurora B inhibition, we employed the specific p38-inhibitor SB202190. The expression of 730 genes was increased at least 2-fold after treatment with ZM447439 (Fig. 1*A*, supplemental data 1, supplemental data 2). A subset of 356 genes required p38 for their induction while the expression of 374 genes was not dependent on p38 (Fig. 1*A*). Genes in both groups include well-known p53 target genes (Fig.

1, *B* and *C*). This indicates that p38-dependent induction of genes by p53 in response Aurora B inhibition is not limited to p21. However, not all p53 target genes require p38 for their full activation. p38-dependent and p38-independent p53 target genes encode for products that are involved in the cellular response to stress, cell cycle arrest, regulation of apoptosis, and the DNA-damage response (Fig. 1, *B* and *C*). RT-qPCR assays of a subset of the identified genes confirmed p38-dependent and -independent regulation of p53-target genes (Fig. 1, *D* and *E*).

Cell Cycle Arrest after Aurora B Inhibition through the E2F/pRB Pathway—In addition to genes up-regulated by ZM447439, 418 genes were down-regulated at least 2-fold after treatment with ZM447439. Interestingly, the expression of 220 genes (53%) was completely or partially restored by co-treatment with SB202190 indicating that their repression requires p38 signaling. These genes may therefore be relevant for p38-dependent cell cycle arrest in response to Aurora B inhibition. A Gene Ontology (GO) analysis of the down-regulated genes whose repression was dependent on p38 revealed that these genes play roles in DNA replication and repair, cell cycle regulation, and mitosis and that many of them are known targets of the pRB/E2F pathway (Fig. 2*A*). RT-qPCR analysis confirmed that the E2F-target genes BLM, RFC3, MCM3, and CCNA2 (cyclin A2) are down-regulated after inhibition of Aurora B, and that their expression was restored when p38-signaling was blocked (Fig. 2*B*).

Down-regulation of E2F-dependent transcription suggested a role for the retinoblastoma protein after inhibition of Aurora B. The p53-target gene p21 functions as a CDK inhibitor and therefore indirectly inhibits phosphorylation of the retinoblastoma (pRB) proteins by CDKs. Expression of p21 thus results in repression of E2F-regulated genes through the formation of repressive pocket-protein/E2F complexes (26). To investigate whether phosphorylation of pRB is indeed reduced after inhibition of Aurora B, we analyzed the phosphorylation pattern of pRB before and after treatment with ZM447439. Inhibition of Aurora B resulted in dephosphorylation of pRB (Fig. 2*C*). pRB dephosphorylation was prevented by SB202190, indicating that p38 signaling is indeed for formation of the active, repressive state of pocket-proteins. To investigate the requirement for p21 induction and for growth arrest after Aurora B inhibition, we generated U2OS cell line stably expressing the SV40 large T (LT) oncogene that binds and inhibits pRB family members and p53. We also used two mutants of LT, LT-K1, and LT-Δ434–444, to test which pathway is involved in p21 induction and growth inhibition. The LT-K1 mutant can no longer bind to and inactivate pRB and thus only targets p53 (27). In contrast, LT-Δ434-444 cannot bind to p53 and only targets pRB and the related pocket proteins p107 and p130 (28). Expression of LT wild type and mutants was verified by immunoblotting (Fig. 2*D*). Expression of all three LT antigens was detectable and not changed after Aurora B inhibition, although expression of LT-Δ434–444 was weaker compared with LT-wild type and LT-K1, as has been observed previously (29). Induction of p21 after inhibition of Aurora B was blocked by wild type LT (Fig. 2*D*). The K1 mutant was also able to block p21 induction while LT-Δ434–444 did not prevent induction of p21. Similarly, siRNA mediated knockdown of pRB also failed to prevent

induction of p21 after treatment with ZM447439 (Fig. 2*E*). These data indicate that p53 but not pRB is required for induction of p21 in response to Aurora B inhibition. Consistent with this finding, p21 was induced after Aurora B inhibition in HCT-116 cells but not in isogenic HCT-116 cells deficient in p53 (Fig. 2*F*) (30). To address the pathways that are required for growth arrest after Aurora B inhibition, Aurora B was inhibited with ZM447439 in U2OS control cells or U2OS-LT, LT-K1 or LT-Δ434–444 cells and cell cycle inhibition was analyzed 24 h later by flow cytometry. After treatment of control cells with ZM447439, an increase of cells with 4N DNA content and a small increase in polyploid cells was detected, consistent with previous studies (Fig. 2*G*) (8–10). When Aurora B was inhibited in cells expressing wild type LT, the fraction of cells >4N and polyploid cells increased strongly, indicating that p53 and/or pRB proteins are required for the cell cycle arrest after Aurora B inhibition. Expression of LT-K1, which still inactivates p53, also resulted in increased polyploidization after ZM447439 treatment, consistent with the finding that p53 is required for p21 induction and with the requirement for p21 in growth inhibition after inhibition of Aurora B (10). Polyploidization was also increased in cells expressing LT-Δ434–444, which only inhibits the retinoblastoma proteins but not p53. Because p21 is induced after Aurora B inhibition in cells expressing LT-Δ434–444 (see Fig. 2*D*), this indicates that the pRB family prevents polyploidization after Aurora B inhibition. Collectively these experiments suggest that inhibition of Aurora B results in cell cycle arrest through p53 and p38-dependent p21 induction, pocket-protein dephosphorylation and inhibition of E2F-dependent transcription.

Inhibition of Aurora B in Interphase Is Not Sufficient for Induction of p21, but Binucleation Is Not Required—The pathways that result in activation of p53 and p21 induction after Aurora B inhibition are incompletely understood. While the mitotic functions of Aurora B are well described, it has been suggested that Aurora B has additional functions in interphase. For example it has recently been reported that Aurora B phosphorylates p53 in interphase resulting in its degradation (22, 23). Conversely, inhibition of Aurora B results in stabilization of p53 and increased transcription of p53 target genes. However, whether Aurora B inhibition in interphase is sufficient to induce p21 has not been addressed. To address this question we arrested cells in G1/S with thymidine and then inhibited Aurora B. Arrest of the cells at the G1/S border was verified by flow cytometry (Fig. 3*B*). Inhibition of Aurora B in G1/S arrested cells with ZM447439 did not result in induction of p21, while p21 was robustly induced in asynchronous cells (Fig. 3*A*). In striking contrast, p21 was strongly induced by ZM447439 when cells were first released from the thymidine-block into mitosis, indicating that inhibition of Aurora B in interphase is not sufficient for activation of p21 (Fig. 3*A*). Although the thymidine-block itself induces some p53 in U2OS cells, p53 was more strongly induced by ZM447439 when cells were released from the thymidine block. Taken together these observations suggest activation of p53 and p21 is a consequence of perturbation of mitosis or cytokinesis.

It has been suggested that p53 is activated by a so-called tetraploidy checkpoint in cells that have undergone mitotic

A

B

C

D

E

F

G
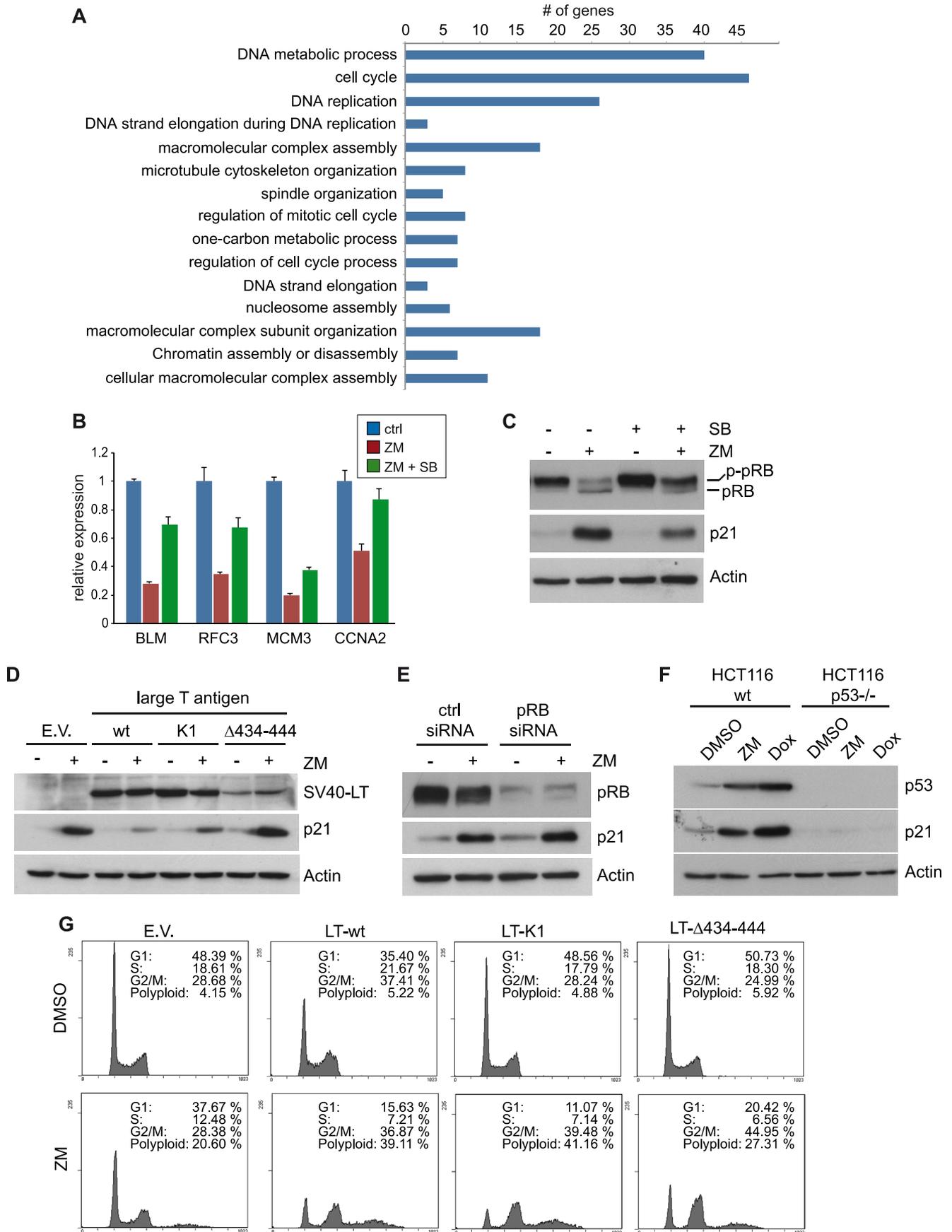
slippage or failed cytokinesis. We therefore next asked whether binucleation as a consequence of cytokinesis failure is required for activation of p53 and p21 when Aurora B is inhibited. To address this question, we treated U2OS cells with different doses of ZM447439 in order to achieve different levels of inhibition of Aurora B and thus different levels of binucleation. Analysis of the phosphorylation status of serine 10 of histone H3, a mitotic substrate of Aurora B, served as a readout for Aurora B inhibition (31). Treatment with 1 μM ZM447439 strongly inhibited Aurora B while a lower dose of 0.5 μM ZM447439 resulted only in partial inhibition of Aurora B (Fig. 3C). 1 μM ZM447439 induced binucleation and accumulation of cells with a 4N DNA content as determined by microscopy and flow cytometry (Fig. 3, D and E). In contrast, partial inhibition with 0.5 μM ZM447439 induced only very few binuclear cells and the fraction of 4N cells did not strongly increase (Fig. 3, D and E). Although partial inhibition of Aurora B did not result in cytokinesis failure, induction of p53 and p21 was observed after treatment with 0.5 μM ZM447439 (Fig. 3F). Importantly, immunofluorescence staining confirmed induction of p21 in mononuclear cells after partial inhibition of Aurora B (Fig. 3G). Low doses of ZM447439 also resulted in induction of p21 in HCT116 cells without inducing binucleation, indicating that induction of p21 in mononucleated cells following inhibition of Aurora B is not specific to aneuploid U2OS cells (data not shown). To confirm that the results are not an artifact of ZM447439 treatment, we validated the results with a second specific Aurora B inhibitor, AZD1152. AZD1152 also activated p21 without binucleation as shown by immuno-staining and immunoblotting (Fig. 3, H and I). We conclude that binucleation and tetraploidy are not necessary for activation of p53 and p21. As described above, we recently demonstrated a specific requirement for p38 MAPK in transcriptional elongation of p21 after Aurora B inhibition (10). We therefore assessed the activation of p38 with an antibody specific for the phosphorylated, active form of p38. We found that p38 is activated after treatment of cells with concentrations of ZM447439 or AZD1152 that do not result in binucleation (Fig. 3, F and H). Taken together these results show that binucleation is not required for induction of p53, p38, and p21.

Increased Aneuploidy Caused by Partial Inhibition of Aurora B Correlates with p21 Induction—It is possible that inhibition of Aurora B induces chromosome segregation defects that are responsible for induction of p53 and p21. To address this possibility we determined the frequency of aneuploidy after treatment of cells with a low concentration of ZM447439 that does not result in binucleation by carrying out interphase FISH assays with probes specific for chromosome 7 and 8. Although U2OS cells are aneuploid with a near trip-

loid status, they show relative low levels of chromosomal instability (32–34). FISH assays with untreated U2OS cells indicated 41% and 3.8% deviation from the mode for chromosome 7 and 8, respectively (Fig. 4, A and B). Upon treatment with 0.5 μM ZM447439 for 24 h, deviation from the mode increased to 65.6% for chromosome 7 and to 14.6% for chromosome 8, indicating that inhibition of Aurora B increases chromosome missegregation and causes changes in the ploidy status of U2OS cells (Fig. 4B). Importantly, inhibition of Aurora B in HCT-116 cells, which are near-diploid, also resulted in aneuploidy as determined by interphase FISH assays with probes specific for chromosome 7 and 8 (Fig. 4, C and D). Taken together, the induction of p53 and p21 in response to Aurora B inhibition correlates with increased chromosomal instability but not with tetraploidization.

Reactive Oxygen Species Are Required for Induction of p21 and for Cell Cycle Arrest in Response to Aurora B Inhibition— Chromosome segregation errors due to partial inhibition of Aurora B could lead to DNA-damage. As DNA-damage is a common activator of p53, we tested for DNA-damage by determining the levels of phosphorylated H2AX (γH2AX). We observed the same low background staining in control-treated and ZM447439-treated cells (Fig. 5A). In contrast, γH2AX positive foci were readily detected in UV-irradiated cells, which was used as a positive control. Lack of a DNA-damage response after Aurora B inhibition was also confirmed by immunoblotting (Fig. 5B). Key regulators of the DNA-damage response are the ATM and ATR kinases (35). Consistent with the absence of γH2AX foci, we could not detect an increase in phosphorylation of ATM and ATR substrates after treatment with 0.5 μM ZM447439 using an antibody that detects endogenous levels of proteins phosphorylated at the ATM/ATR substrate motif (Fig. 5C). Importantly, a positive result was obtained after doxorubicin induced DNA-damage (Fig. 5C). Furthermore, the ATR and ATM kinase inhibitors VE-821 and KU5593 did not prevent induction of p21 after Aurora B inhibition, indicating that these kinases are not required for activation of p21 after partial inhibition of Aurora B (Fig. 5D). In fact, p21 expression was slightly induced by high concentrations of KU5596 or VE-821. After induction of DNA-damage with doxorubicin, KU5593 and VE-821 prevented phosphorylation of Chk1 and Chk2, respectively, confirming the specificity of the ATM and ATR inhibitors (Fig. 5E).

Aneuploid MEFs have an increased glucose metabolism resulting in high levels of reactive oxygen species (ROS) (36) We therefore speculated that aneuploidy due to partial inhibition of Aurora B could result in increased ROS production. Indeed, cells accumulated significant levels of intracellular lev-

FIGURE 2. **Cell cycle arrest after Aurora B inhibition is mediated by inhibition of E2F-dependent transcription.** *A*, GO analysis of genes down-regulated by ZM447439 in a p38-dependent manner. Listed are the top fifteen overrepresented GO terms according to the *p* value. *B*, validation of p38-dependent repression of E2F-targets. U2OS cells were treated as described in Fig. 1. mRNA levels of the indicated E2F-target genes were determined by RT-qPCR. *C*, U2OS cells were treated as in Fig. 1 and lysates were subjected to immunoblotting with the indicated antibodies. *pRB*: hypophosphorylated pRB; *p-pRB*: phosphorylated pRB. *D*, U2OS cells expressing empty vector (E.V.) or SV40 large T antigen (wild type, K1 or Δ434–444) were treated with DMSO or 1 μM ZM447439 for 24 h. Expression of SV 40 Large T antigen and p21 was analyzed by immunoblotting. *β*-Actin served as a loading control. *E*, U2OS cells transfected with control siRNA or pRB-specific siRNA were treated with 1 μM ZM447439 for 24 h. Expression of pRB and p21 was determined by immunoblotting. *β*-Actin served as a loading control. *F*, HCT116 wild type or HCT116 p53$^{-/-}$ cells were treated with DMSO, 1 μM ZM447439 or 1 μM doxorubicin for 24 h and the induction of p53 and p21 was analyzed by immunoblotting. *β*-Actin served as a loading control. *G*, indicated cell lines were treated with either DMSO or 1 μM ZM447439 for 24 h. Flow cytometry was performed to determine the fraction of cells in the different phases of the cell cycle.
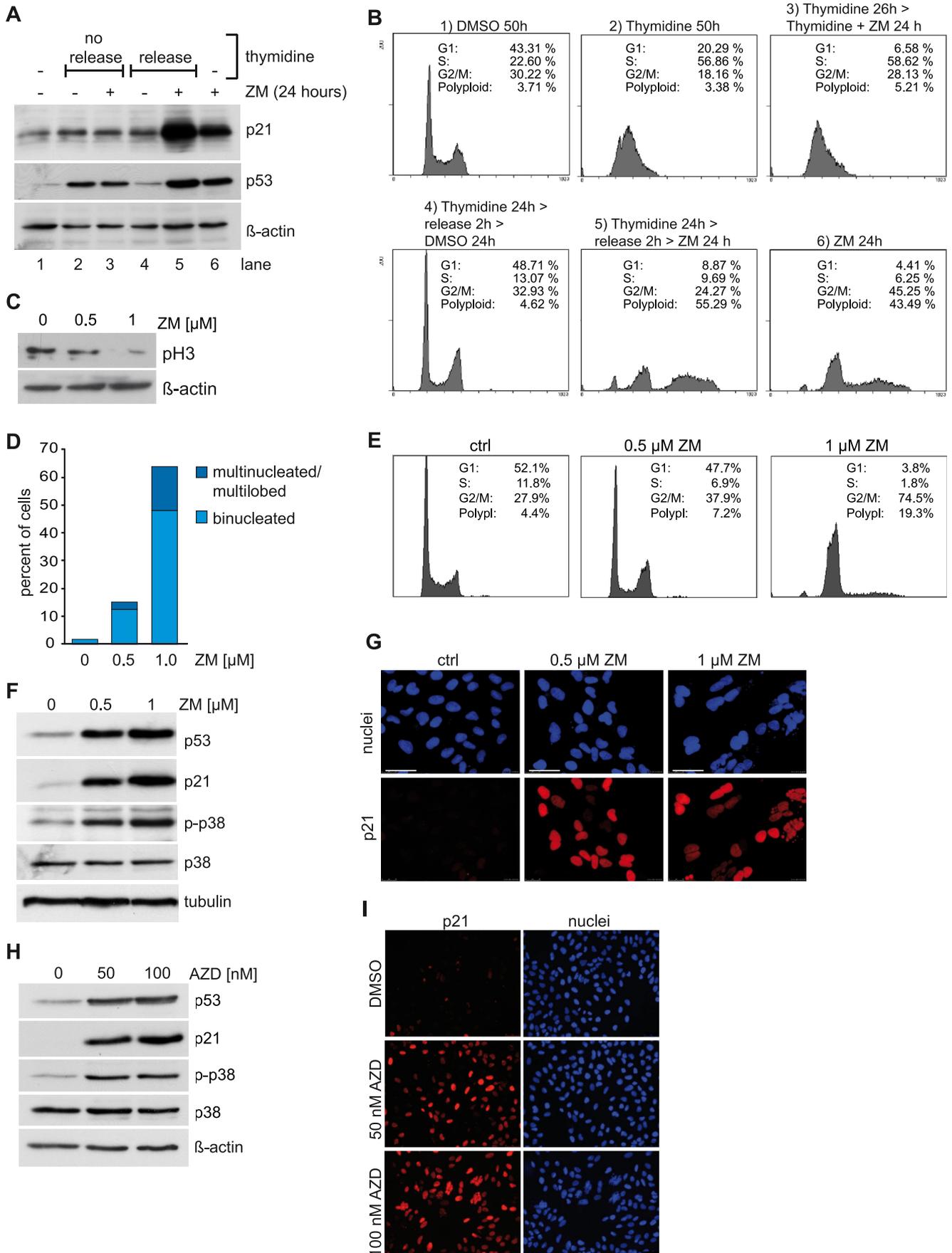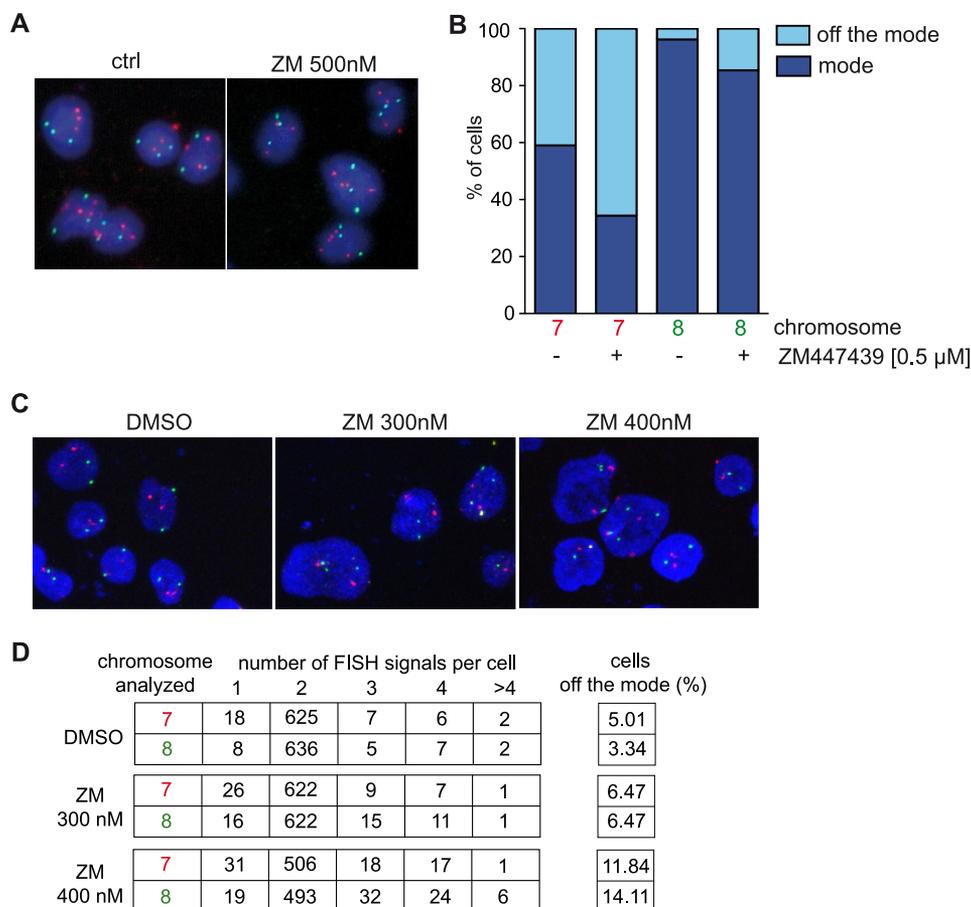
FIGURE 4. Aneuploidy after partial inhibition of Aurora B. *A*, example microphotographs of interphase FISH assays of control U2OS cells or cells treated with 0. 5 μM ZM447439. Chromosome 7: *red*; chromosome 8: *green*. *B*, quantification of interphase FISH signals for chromosomes 7 and 8 in control and 0.5 μM ZM447349-treated U2OS cells. *C*, example microphotographs of interphase FISH assays of control HCT116 cells or cells treated with 0.3 μM or 0.4 μM ZM447439 for 48 h. Chromosome 7: *red*; chromosome 8: *green*. *D*, quantification of interphase FISH signals for chromosomes 7 and 8 in control and ZM447349-treated HCT116 cells shown in *C*. The difference in the percentage of cell off the mode after treatment with 400 nM ZM447439 was statistically significant (chromosome 7 or 8 *p* values <0.001). With 300 nM ZM447439 the difference in percentage of cells of the mode was not significant for chromosome 7 but was significant for chromosome 8 (*p* = 0.009). A chi-squared test was used to analyze the data.

els of ROS after inhibition of Aurora B compared with control-treated cells, as determined with the general oxidative stress indicator H2-DCFDA (Fig. 6*A*). Furthermore, using the fluorescence dye MitoSox Red, an increase in mitochondrial superoxide production was observed after ZM447439-treatment (Fig. 6*B*). These observations suggest that p21 might be induced by ROS generated in aneuploid cells. To test whether activation of p53 and induction of p21 depends on ROS production, we co-treated ZM447439 cells with the antioxidant 4,5-dihydroxy-benzene-1,3-disulfonate (Tiron), a superoxide anion scavenger. Tiron suppressed the production of superoxide as determined with MitoSox Red (Fig. 6*B*). Importantly, Tiron also suppressed

the induction of p21 by ZM447439 (Fig. 6*C*). Tiron also prevented the activation of p38 and it had a partial effect on the induction of p53 (Fig. 6*C*). Furthermore, the down-regulation of the E2F-regulated genes B-MYB, cyclin A and E2F1 by ZM447439 was also rescued by co-treatment with Tiron (Fig. 6*C*, *bottom panels*). These observations support the idea that ROS functions upstream of p38 and p21 in aneuploid cells after partial inhibition of Aurora B. Next we asked whether ROS is required to inhibit entry into S-phase in response to Aurora B inhibition. To address this question we measured DNA-synthesis by BrdU incorporation. As expected, DNA synthesis was inhibited by ZM447439 (Fig. 6, *D* and *E*). Importantly, BrdU

FIGURE 3. p21 induction without binucleation after Aurora B inhibition. *A*, U2OS cells were synchronized in G1/S by treatment with 2.5 mM thymidine for 24 h (*lanes 2–5*). Thymidine-blocked cells were treated with DMSO or with 1 μM ZM447439 for 24 h either without release (*lanes 2* and *3*) or after a 2-hour release from the thymidine block (*lanes 4* and *5*). Asynchronous cells (*lane 1*) and asynchronous cells treated with 1 μM ZM447439 for 24 h (*lane 6*) served as controls. Levels of p21 and p53 were determined by immunoblotting. β-Actin served as a loading control. *B*, cell cycle synchronization of the experiment shown in *A* was confirmed by flow cytometry. *C*, U2OS cells were treated with 0.5 μM or 1 μM ZM447439 for 24 h. Histone H3 phosphorylated at serine 10 (pH3) was analyzed by immunoblotting. β-Actin served as a loading control. *D*, U2OS cells were treated as described in *C* and analyzed by fluorescence microscopy. The fraction of bi- and multinucleated and multilobed cells was determined. More than 300 cells were counted. *E*, fraction of cells in different phases of the cell cycle in the experiment shown in *C* was determined by FACS. *F*, levels of p53, p21, p38, and phosphorylated p38 (p-p38) in U2OS cells treated with 0.5 μM or 1 μM ZM447439 for 24 h, were determined by immunoblotting. Tubulin served as loading control. *G*, U2OS cells were treated with 0.5 μM or 1 μM ZM447439 for 24 h. The level of p21 was determined by immunostaining. DNA was counterstained with Hoechst 33258. Bar: 50 μm. *H*, U2OS cells were treated with 50 nM or 100 nM AZD1152 for 24 h. p21, p38, p-p38, and p53 levels were determined by immunoblotting β-actin served as a loading control. *I*, U2OS cells were treated as in *H*. Levels of p21 were analyzed by immunostaining. DNA was counterstained with Hoechst 33258.
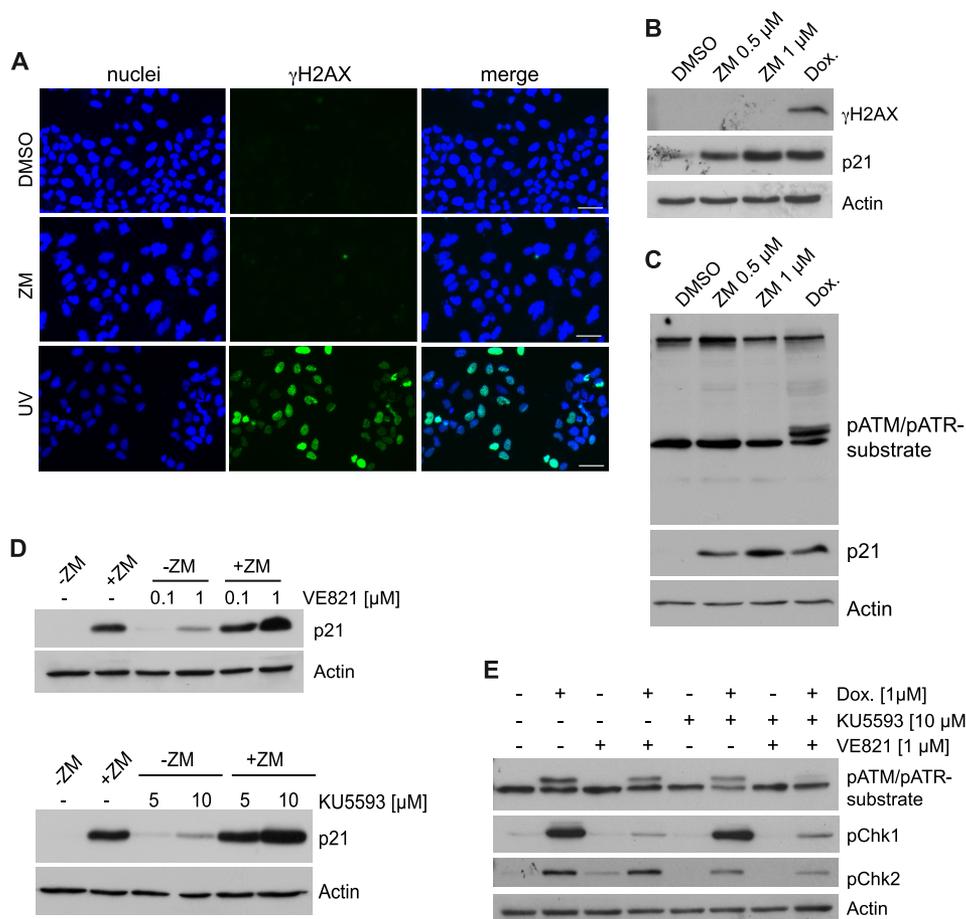
FIGURE 5. **The DNA-damage response is not involved in induction of p21 after partial inhibition of Aurora B.** *A*, U2OS cells were treated with DMSO, 0.5 μM ZM447439 for 24 h or irradiated with UV-light (10J/m^2). γH2AX foci were detected by immunostaining. DNA was counterstained with Hoechst 33258. Bar: 50 μm. *B*, U2OS cells were treated with 0.5 μM or 1 μM ZM447439 for 24 h or with 1 μM doxorubicin for 6 h. Levels of γH2AX and p21 were determined by immunoblotting. *C*, U2OS cells were treated with DMSO, 1 μM ZM447439 for 24 h or with 1 μM doxorubicin (*Dox.*) for 6 h. Levels of phosphorylated ATM/ATR substrates and p21 were detected by immunoblotting. β-Actin served as a control. *D*, U2OS cells were pretreated with the indicated concentration of VE-821 (*upper panels*) or KU5593 (*lower panels*) for 2 h and then treated with 1 μM ZM447439 for 24 h. p21 levels were determined by immunoblotting. β-actin served as a control. *E*, U2OS cells were pretreated with 1 μM VE-821 or 10 μM KU5593 for 2 h and then treated with 1 μM doxorubicin (*Dox.*) for 6 h. pChk1 and pChk2 levels and levels of phosphorylated ATM/ATR substrates were determined by immunoblotting. β-Actin served as a control.

incorporation was almost completely restored by co-treatment with Tiron, indicating that ROS is required for G1 arrest in response to Aurora B inhibition (Fig. 6, *D* and *E*).

Aurora B Inhibition Synergizes with Drugs that Act Specifically on Aneuploid Cells—It has been reported that aneuploid cells are sensitive to a variety of compounds including the heat shock protein 90 (Hsp90) inhibitor 17-AAG and AICAR, an activator of the AMP-activated protein kinase (AMPK) (37). Given that inhibition of Aurora B was sufficient to induce aneuploidy, we next asked whether drugs that target aneuploidy synergize with Aurora B inhibitors. To address this possibility, HCT116 and U2OS cells were plated at low density and treated with AICAR or 17-AAG in the presence or absence of ZM447439. The number of colonies was determined after 14 days by crystal violet staining. Treatment of U2OS or HCT-116 with low doses of ZM447439 did not inhibit colony formation when used alone (Fig. 7*A*). Similarly, 17-AAG had little effect on colony formation while AICAR had a modest inhibitory effect (Fig. 7*A*). In striking contrast, when cells were treated with a combination of AICAR and ZM447439 or with 17-AAG and ZM447439, colony formation was strongly inhibited (Fig.

7*A*). The synergy between ZM447438 and AICAR and between ZM447439 and 17-AAG was confirmed by extracting the dye and quantification of the absorbance (Fig. 7*B*). Co-treatment of ZM447439 with 17-AAG or AICAR did not result in apoptosis or senescence as determined by FACS using Annexin V staining and by staining for senescence-associated β-galactosidase activity. This suggests that these processes are not responsible for the observed synergistic effect (data not shown). However, we found a synergistic increase in p21 levels at early time points of drug co-treatment compared with treatment with ZM447439 alone (Fig. 7*C*), which could account for the reduced colony formation.

We next investigated whether co-treatment with ZM447439 and AICAR, which more strongly synergized with ZM447439 than 17-AAG in HCT116 cells, inhibits oncogenic transformation. To do so, we determined the ability to grow independently of anchorage in soft agar. Control-treated HCT116 cells readily formed colonies in soft agar when seeded at low density (Fig. 7*D*). Treatment with either AICAR or ZM447439 had no effect on colony formation. In contrast, co-treatment with AICAR and ZM447439 led to a significant decrease in growth in soft
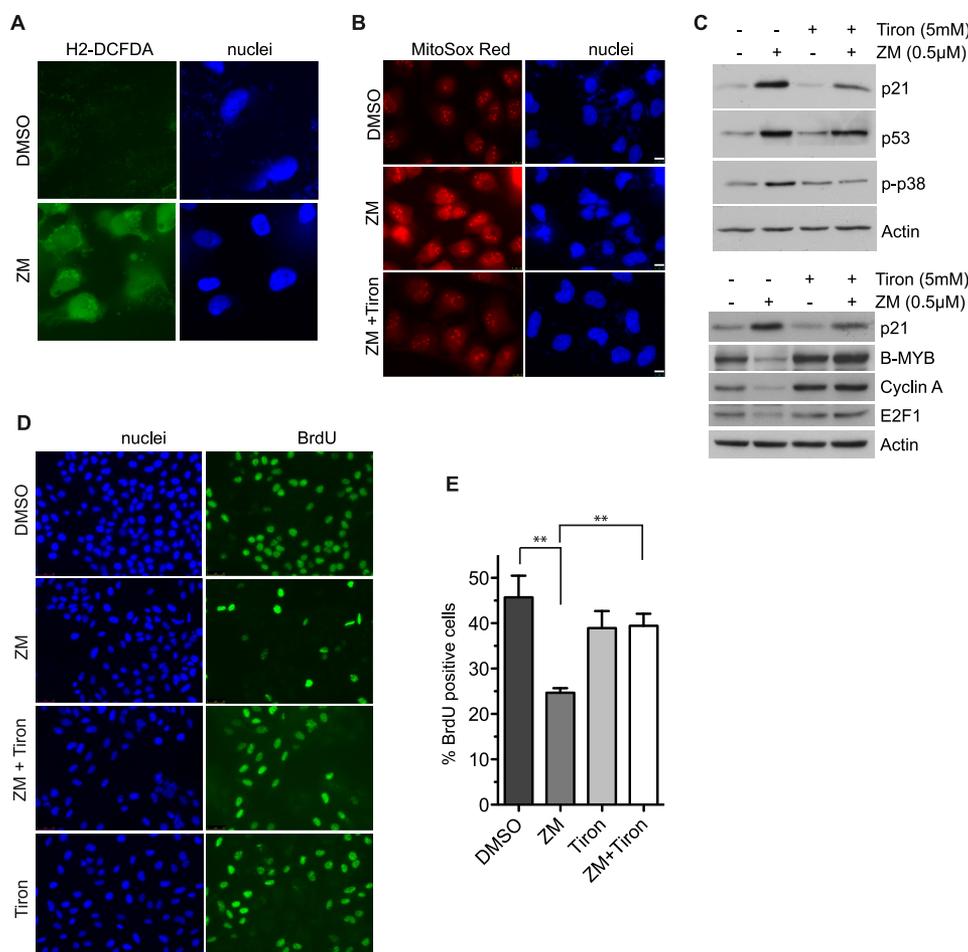
FIGURE 6. **Reactive oxygen species are required for induction of p21 and for cell cycle arrest in response to Aurora B inhibition.** *A*, detection of ROS with the fluorescent dye H2DFC-DA in U2OS cells treated with DMSO or 0.5 μM ZM447439 for 24 h. DNA was counterstained with Hoechst 33258. *B*, ROS generation was analyzed with MitoSox Red in U2OS cells treated with DMSO, 0.5 μM ZM447439, or co-treated with 0.5 μM ZM447439 and 5 mM Tiron for 24 h. DNA was counterstained with Hoechst 33342. Bar 10 μm. *C*, U2OS cells were treated as in *B*. Levels of the indicated proteins were determined by immunoblotting. β-Actin served as a control. *D*, U2OS cells were treated for 48 h with DMSO, 0.5 μM ZM447439, 5 mM Tiron or co-treated with 0.5 μM ZM447439 and 5 mM Tiron. Cells were pulse labeled with 15 μg/ml BrdU for 2 h. BrdU was detected by immunofluorescence. DNA was counterstained with Hoechst 33258. *E*, percentage of BrdU-positive cells shown in *D* was determined. Error bars represent standard deviation of four independent experiments. The differences between DMSO and ZM447439 ($p = 0.005$) and between ZM447439 and ZM44749 + Tiron ($p = 0.0019$) were statistically significant (Student's *t* test).

agar. Taken together these data indicate that inhibition of Aurora B synergizes with drugs specifically acting on aneuploid cells (AICAR and 17AAG) to inhibit cell growth and transformation.

DISCUSSION

In this study, we investigated the regulation of p21 and the requirements for growth arrest in response to inhibition of Aurora B. Our findings are summarized in Fig. 8. We demonstrate that inhibition of Aurora B in interphase is not sufficient for induction of p21 but that progression through mitosis is required. This suggests that aberrations in mitosis are responsible for induction of p21. Our finding is inconsistent with a recent study using conditional knock-out MEFs that reported induction of p21 after ablation of Aurora B in quiescent cells (21). It is possible that the requirements for p21 activation are different in primary mouse cells and human cell lines. It will therefore be important to investigate whether this requirement is specific to human cell lines.

We further present evidence that induction of p21 does not require changes in ploidy and that p21 is induced in mononu-

cleated cells after partial inhibition of Aurora B. Complete inhibition of Aurora B leads to premature exit from mitosis without cell division as a result of cytokinesis failure (7). It was proposed that a tetraploidy-checkpoint detects the increase in chromosome number and arrests the cells in a tetraploid G1 state via activation of p53 and p21. However, the concept of a true tetraploidy-checkpoint has recently been challenged. Other possibilities that have been proposed to mediate a cell cycle arrest after an aberrant mitosis include DNA-damage, centrosomal stress or activation of p53 by the lack of transcription during prolonged mitosis (18–20). Activation of p21 in mononucleated cells after incomplete inhibition of Aurora B indicates that mitotic stress and not tetraploidy is responsible for p53 and p21 activation. Similar findings were reported recently using different experimental approaches. For example, an inhibitor of the mitotic kinesin Eg5 resulted in chromosome missegregation and in activation p53 (38). Similarly, p53 was activated by aneuploidy in SAC-deficient cells (36).

We further demonstrate that induction of p21 after inhibition of Aurora B is independent of DNA-damage but involves increased levels of ROS. A role for ROS in induction of p21 is
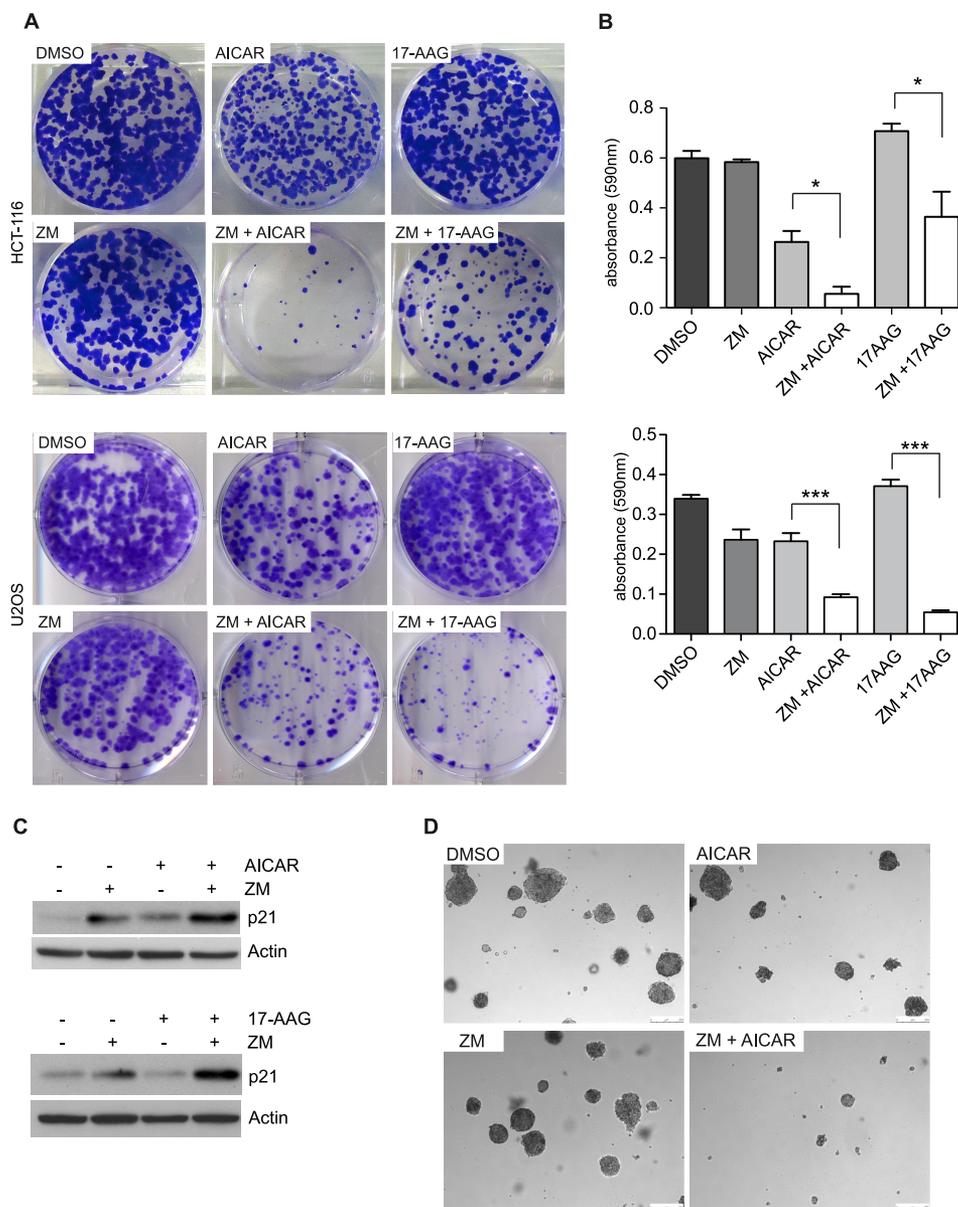
FIGURE 7. **Drugs that target aneuploid cells synergize with inhibition of Aurora B.** *A*, HCT116 or U2OS cells were treated with DMSO, AICAR (200 μM), 17-AAG (8 nM), ZM447439 (0.4 μM for HCT116 cells, and 0.5 μM for U2OS cells) or a combination of ZM447439 with AICAR or 17-AAG. 14 days later, colonies were fixed and stained with crystal violet. *B*, quantification of the colony forming assay shown in *A*. The dye was extracted, and absorbance (at 590 nm) was determined. The experiment was performed in triplicates. Error bars represent standard deviation. *C*, U2OS cells were treated with DMSO, AICAR (200 μM), 17-AAG (8 nM), ZM447439 (0.5 μM) or a combination of ZM447439 with AICAR or 17AAG for 12 h. Levels of p21 were determined by immunoblotting. *D*, soft agar assays were performed to analyze anchorage independent growth of HCT116 cells treated with DMSO, AICAR (200 μM, ZM447439 (0.4 μM), or a combination of ZM447439 and AICAR.

supported by the observation that the response was suppressed by treatment with the ROS scavenger Tiron. The production of ROS might be triggered by an altered energy metabolism and by proteotoxic stress experienced by aneuploid cells. Increased ROS levels have also been detected in aneuploid cells generated by defects in the spindle checkpoint (36). Proteotoxic stress after Aurora B inhibition could be a consequence of the imbalance in protein synthesis for the genes encoded on aneusomic chromosomes as it has been observed in several recent studies using aneuploid yeast and mammalian cell culture models (37, 39–41).

How does ROS lead to the induction of p21? Our previous studies have implicated p38 MAPK signaling in induction of

p21 after inhibition of Aurora B (10). Specifically, we have shown that p38 MAPK is not required for binding of p53 to the p21 promoter but acts subsequent to p53 binding to promote transcriptional elongation of p21 by RNA polymerase II (10). Because p38 MAPK is activated after Aurora B inhibition in a ROS dependent manner, collectively these data suggest a model in which inhibition of Aurora B results in production of ROS and this in turn leads to activation of p38 which then mediates the p21-induction via stimulating its transcriptional elongation (see Fig. 8). A possible mechanism for activation of p38 by ROS is via inhibition of MAPK phosphatases. It has been shown that MAPK phosphatases are inhibited by ROS through oxidation of critical cysteine residues in the catalytic domain leading to acti-
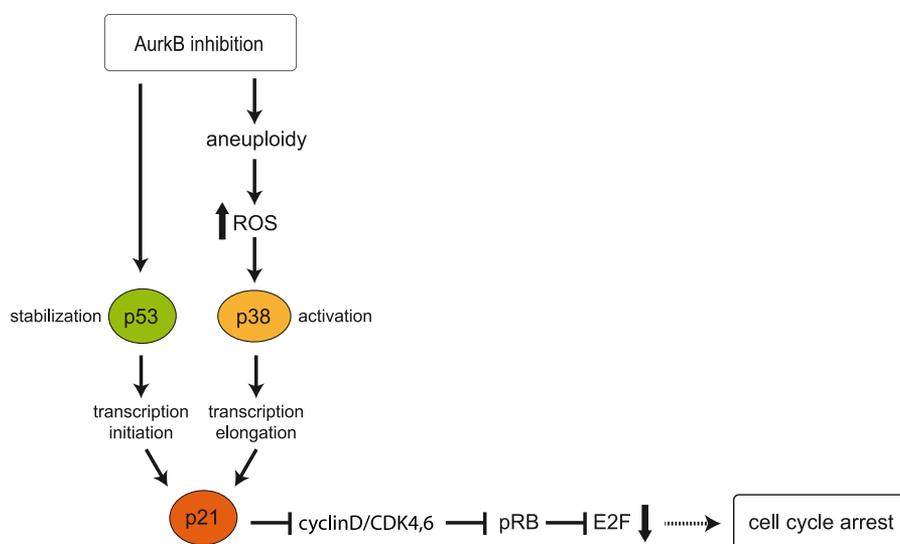
FIGURE 8. **Summary and model.** p53 is stabilized when Aurora B is inhibited (22, 23). Aurora B inhibition also results in chromosome missegregation and aneuploidy, triggering the production of ROS, which leads to p38 activation. p38 is required transcriptional elongation of the p21 mRNA (10). p21 mediates dephosphorylation and activation of pRB resulting in inhibition of E2F-dependent transcription and in cell cycle arrest.

vation of p38 (42). Additional studies are necessary to determine whether MAPK phosphatases are involved in activation of p38 upon Aurora B inhibition.

Our microarray studies showed that the p38-dependent activation of genes after Aurora B inhibition regulation is not limited to p21, and that a subset of p53 regulated genes require p38 signaling for their activation. One example of a gene that is activated in a p38-dependent manner is ATF3, which known to be regulated at the level of transcriptional elongation in response to stress (43). It was reported that transcriptional elongation of ATF3 depends on Elongin A, a subunit of a multimeric complex that activates elongation by mammalian RNA Polymerase II (44). It remains to be shown whether other genes that are induced in a p38-dependent manner are also regulated on the level of transcriptional elongation and whether Elongin A is involved in their regulation.

Aurora B inhibition is also associated with a decrease in E2F-dependent transcription and in dephosphorylation of pRB. This suggests that the cell cycle arrest is mediated by formation of repressive pocket-protein/E2F complexes and down-regulation of E2F-dependent gene expression. This conclusion is supported by the finding that cell cycle inhibition was overcome by expression of a mutant SV40 large T oncogene that only inhibits pRB family members but not p53 (Fig. 2). It has previously been shown that Aurora B phosphorylates pRB (24). Thus Aurora B could directly affect the function of pRB. However, we observed that pRB-dephosphorylation upon Aurora B inhibition was prevented when p38-signaling was blocked. This suggests an indirect mode of pRB regulation through p21 and inhibition of CDK activity. Thus, pRB is not a direct target of Aurora B, at least in the cell lines studied here.

Aurora kinases are overexpressed in many human cancers and they are potential therapeutic targets (45, 46). Although some Aurora kinase inhibitors worked well in *in vitro* studies, they performed relatively poorly in clinical trials (47). Based on our observation that drugs which acts on the cellular energy metabolism or on the proteome strongly synergized with par-

tial Aurora B inhibition, we suggest that the aneuploidy induced by partial Aurora B inhibition can be exploited therapeutically by combining Aurora B inhibitors with compounds such as AICAR or 17-AAG. It will be important to validate this concept in future studies *in vivo* mouse tumor models.

REFERENCES

1. Gordon, D. J., Resio, B., and Pellman, D. (2012) Causes and consequences of aneuploidy in cancer. *Nat. Rev. Genet.* **13,** 189 – 203
2. Carmena, M., Wheelock, M., Funabiki, H., and Earnshaw, W. C. (2012) The chromosomal passenger complex (CPC): from easy rider to the godfather of mitosis. *Nat. Rev. Mol. Cell Biol.* **13,** 789 – 803
3. Vader, G., and Lens, S. M. A. (2008) The Aurora kinase family in cell division and cancer. *Biochim. Biophys. Acta* **1786,** 60 – 72
4. Ruchaud, S., Carmena, M., and Earnshaw, W. C. (2007) Chromosomal passengers: conducting cell division. *Nat. Rev. Mol. Cell Biol.* **8,** 798 – 812
5. Earnshaw, W. C., and Cooke, C. A. (1991) Analysis of the distribution of the INCENPs throughout mitosis reveals the existence of a pathway of structural changes in the chromosomes during metaphase and early events in cleavage furrow formation. *J. Cell Sci.* **98,** 443 – 461
6. Vader, G., Medema, R. H., and Lens, S. M. A. (2006) The chromosomal passenger complex: guiding Aurora-B through mitosis. *J. Cell Biol.* **173,** 833 – 837
7. Ditchfield, C., Johnson, V. L., Tighe, A., Ellston, R., Haworth, C., Johnson, T., Mortlock, A., Keen, N., and Taylor, S. S. (2003) Aurora B couples chromosome alignment with anaphase by targeting BubR1, Mad2, and Cenp-E to kinetochores. *J. Cell Biol.* **161,** 267 – 280
8. Gizatullin, F., Yao, Y., Kung, V., Harding, M. W., Loda, M., and Shapiro, G. I. (2006) The Aurora kinase inhibitor VX-680 induces endoreduplication and apoptosis preferentially in cells with compromised p53-dependent postmitotic checkpoint function. *Cancer Res.* **66,** 7668 – 7677
9. Dreier, M. R., Grabovich, A. Z., Katusin, J. D., and Taylor, W. R. (2009) Short and long-term tumor cell responses to Aurora kinase inhibitors. *Exp. Cell Res.* **315,** 1085 – 1099
10. Kumari, G., Ulrich, T., and Gaubatz, S. (2013) A role for p38 in transcriptional elongation of p21 (CIP1) in response to Aurora B inhibition. *Cell Cycle* **12,** 2051 – 2060

11. Gomes, N. P., Bjerke, G., Llorente, B., Szostek, S. A., Emerson, B. M., and Espinosa, J. M. (2006) Gene-specific requirement for P-TEFb activity and RNA polymerase II phosphorylation within the p53 transcriptional program. *Genes Dev.* **20,** 601–612

12. Espinosa, J. M., Verdun, R. E., and Emerson, B. M. (2003) p53 functions through stress- and promoter-specific recruitment of transcription initiation components before and after DNA damage. *Mol. Cell* **12,** 1015–1027

13. Valin, A., Ouyang, J., and Gill, G. (2013) Transcription factor Sp3 represses expression of p21CIP1 via inhibition of productive elongation by RNA Polymerase II. *Mol. Cell Biol.* **33,** 1582–1593

14. Andreassen, P. R., Lohez, O. D., Lacroix, F. B., and Margolis, R. L. (2001) Tetraploid state induces p53-dependent arrest of nontransformed mammalian cells in G1. *Mol. Biol. Cell* **12,** 1315–1328

15. Margolis, R. L., Lohez, O. D., and Andreassen, P. R. (2003) G1 tetraploidy checkpoint and the suppression of tumorigenesis. *J. Cell Biochem.* **88,** 673–683

16. Wong, C., and Stearns, T. (2005) Mammalian cells lack checkpoints for tetraploidy, aberrant centrosome number, and cytokinesis failure. *BMC Cell Biol.* **6,** 6

17. Uetake, Y. (2004) Cell cycle progression after cleavage failure: mammalian somatic cells do not possess a "tetraploidy checkpoint." *J. Cell Biol.* **165,** 609–615

18. Blagosklonny, M. V. (2006) Prolonged mitosis versus tetraploid checkpoint: how p53 measures the duration of mitosis. *Cell Cycle* **5,** 971–975

19. Dalton, W. B., Nandan, M. O., Moore, R. T., and Yang, V. W. (2007) Human cancer cells commonly acquire DNA damage during mitotic arrest. *Cancer Res.* **67,** 11487–11492

20. Quignon, F., Rozier, L., Lachages, A.-M., Bieth, A., Simili, M., and Debatisse, M. (2007) Sustained mitotic block elicits DNA breaks: one-step alteration of ploidy and chromosome integrity in mammalian cells. *Oncogene* **26,** 165–172

21. Trakala, M., Fernández-Miranda, G., Pérez de Castro, I., Heeschen, C., and Malumbres, M. (2013) Aurora B prevents delayed DNA replication and premature mitotic exit by repressing p21 (Cip1). *Cell Cycle* **12,** 1030–1041

22. Gully, C. P., Velazquez-Torres, G., Shin, J.-H., Fuentes-Mattei, E., Wang, E., Carlock, C., Chen, J., Rothenberg, D., Adams, H. P., Choi, H. H., Guma, S., Phan, L., Chou, P.-C., Su, C.-H., Zhang, F., Chen, J.-S., Yang, T.-Y., Yeung, S.-C. J., and Lee, M.-H. (2012) Aurora B kinase phosphorylates and instigates degradation of p53. *Proc. Natl. Acad. Sci. U.S.A.* **109,** E1513–22

23. Wu, L., Ma, C. A., Zhao, Y., and Jain, A. (2011) Aurora B interacts with NIR-p53, leading to p53 phosphorylation in its DNA-binding domain and subsequent functional suppression. *J. Biol. Chem.* **286,** 2236–2244

24. Nair, J. S., Ho, A. L., Tse, A. N., Coward, J., Cheema, H., Ambrosini, G., Keen, N., and Schwartz, G. K. (2009) Aurora B kinase regulates the post-mitotic endoreduplication checkpoint via phosphorylation of the retinoblastoma protein at serine 780. *Mol. Biol. Cell* **20,** 2218–2228

25. Marxer, M., Ma, H. T., Man, W. Y., and Poon, R. Y. C. (2013) p53 deficiency enhances mitotic arrest and slippage induced by pharmacological inhibition of Aurora kinases. *Oncogene* doi: 10.1038/onc.2013.325

26. Polager, S., and Ginsberg, D. (2009) p53 and E2f: partners in life and death. *Nat. Rev. Cancer* **9,** 738–748

27. Zalvide, J., and DeCaprio, J. A. (1995) Role of pRb-related proteins in simian virus 40 large-T-antigen-mediated transformation. *Mol. Cell Biol.* **15,** 5800–5810

28. Kierstead, T. D., and Tevethia, M. J. (1993) Association of p53 binding and immortalization of primary C57BL/6 mouse embryo fibroblasts by using simian virus 40 T-antigen mutants bearing internal overlapping deletion mutations. *J. Virol.* **67,** 1817–1829

29. Ye, X., Zerlanko, B., Zhang, R., Somaiah, N., Lipinski, M., Salomoni, P., and Adams, P. D. (2007) Definition of pRB- and p53-dependent and -independent steps in HIRA/ASF1a-mediated formation of senescence-associated heterochromatin foci. *Mol. Cell Biol.* **27,** 2452–2465

30. Bunz, F., Dutriaux, A., Lengauer, C., Waldman, T., Zhou, S., Brown, J. P., Sedivy, J. M., Kinzler, K. W., and Vogelstein, B. (1998) Requirement for p53 and p21 to sustain G2 arrest after DNA damage. *Science* **282,** 1497–1501

31. Hirota, T., Lipp, J. J., Toh, B.-H., and Peters, J.-M. (2005) Histone H3 serine 10 phosphorylation by Aurora B causes HP1 dissociation from heterochromatin. *Nature* **438,** 1176–1180

32. Al-Romaih, K., Bayani, J., Vorobyova, J., Karaskova, J., Park, P. C., Zielenska, M., and Squire, J. A. (2003) Chromosomal instability in osteosarcoma and its association with centrosome abnormalities. *Cancer Genet. Cytogenet.* **144,** 91–99

33. Bayani, J., Zielenska, M., Pandita, A., Al-Romaih, K., Karaskova, J., Harrison, K., Bridge, J. A., Sorensen, P., Thorner, P., and Squire, J. A. (2003) Spectral karyotyping identifies recurrent complex rearrangements of chromosomes 8, 17, and 20 in osteosarcomas. *Genes Chromosomes Cancer* **36,** 7–16

34. Bakhoum, S. F., Thompson, S. L., Manning, A. L., and Compton, D. A. (2009) Genome stability is ensured by temporal control of kinetochore-microtubule dynamics. *Nat. Cell Biol.* **11,** 27–35

35. Cimprich, K. A., and Cortez, D. (2008) ATR: an essential regulator of genome integrity. *Nat. Rev. Mol. Cell Biol.* **9,** 616–627

36. Li, M., Fang, X., Baker, D. J., Guo, L., Gao, X., Wei, Z., Han, S., van Deursen, J. M., and Zhang, P. (2010) The ATM-p53 pathway suppresses aneuploidy-induced tumorigenesis. *Proc. Natl. Acad. Sci. U.S.A.* **107,** 14188–14193

37. Tang, Y.-C., Williams, B. R., Siegel, J. J., and Amon, A. (2011) Identification of aneuploidy-selective antiproliferation compounds. *Cell* **144,** 499–512

38. Thompson, S. L., and Compton, D. A. (2010) Proliferation of aneuploid human cells is limited by a p53-dependent mechanism. *J. Cell Biol.* **188,** 369–381

39. Torres, E. M., Sokolsky, T., Tucker, C. M., Chan, L. Y., Boselli, M., Dunham, M. J., and Amon, A. (2007) Effects of aneuploidy on cellular physiology and cell division in haploid yeast. *Science* **317,** 916–924

40. Oromendia, A. B., Dodgson, S. E., and Amon, A. (2012) Aneuploidy causes proteotoxic stress in yeast. *Genes Dev.* **26,** 2696–2708

41. Pavelka, N., Rancati, G., Zhu, J., Bradford, W. D., Saraf, A., Florens, L., Sanderson, B. W., Hattem, G. L., and Li, R. (2010) Aneuploidy confers quantitative proteome changes and phenotypic variation in budding yeast. *Nature* **468,** 321–325

42. Kamata, H., Honda, S.-I., Maeda, S., Chang, L., Hirata, H., and Karin, M. (2005) Reactive oxygen species promote TNFα-induced death and sustained JNK activation by inhibiting MAP kinase phosphatases. *Cell* **120,** 649–661

43. Kawauchi, J., Inoue, M., Fukuda, M., Uchida, Y., Yasukawa, T., Conaway, R. C., Conaway, J. W., Aso, T., and Kitajima, S. (2013) Transcriptional properties of mammalian Elongin A and its role in stress response. *J. Biol. Chem.* **288,** 24302–24315

44. Aso, T., Lane, W. S., Conaway, J. W., and Conaway, R. C. (1995) Elongin (SIII): a multisubunit regulator of elongation by RNA polymerase II. *Science* **269,** 1439–1443

45. Keen, N., and Taylor, S. (2004) Aurora-kinase inhibitors as anticancer agents. *Nat. Rev. Cancer* **4,** 927–936

46. Katayama, H., and Sen, S. (2010) Aurora kinase inhibitors as anticancer molecules. *Biochim. Biophys. Acta* **1799,** 829–839

47. Boss, D. S., Beijnen, J. H., and Schellens, J. H. M. (2009) Clinical experience with aurora kinase inhibitors: a review. *Oncologist* **14,** 780–793